Crystal structure of an antiparallel DNA fragment with Hoogsteen base pairing

Nicola G. A. Abrescia*†, Andrew Thompson‡, Tam Huynh-Dinh§, and Juan A. Subirana*¶

*Departament d'Enginyeria Química, Universitat Politècnica de Catalunya, Avga Diagonal 647, E-08028 Barcelona, Spain; ‡European Synchrotron Radiation Facility, BP 220, F-38043 Grenoble, France; and §Unité de Chimie Organique, Institut Pasteur, 28 rue du Docteur Roux, F-75724 Paris, France

Communicated by Ignacio Tinoco, Jr., University of California, Berkeley, CA, December 17, 2001 (received for review October 29, 2001)

We report here an alternative double-helical structure of the DNA molecule. It has been found in the d(ATA^{Br}UAT) and d(ATATAT) sequences by single-crystal x-ray crystallography. This sequence is found not only in TATA boxes, but also in other regulatory regions of DNA. Bases of the two antiparallel strands form Hoogsteen pairs, with adenines in the *syn* conformation. The structure is related neither to those found in triple helices nor to parallel DNA duplexes. Its conformational parameters are very similar to those of duplex DNA in the B form. Both forms may coexist under physiological conditions, although the Hoogsteen pairing greatly influences the recognition sites on DNA. Our results demonstrate that an alternative to the classical B-DNA double helix is possible.

The biological relevance of AT-rich regions of DNA in molecular processes is well known (1–4). The promoter sequences of many eukaryotic structural genes are composed of stretches of adenine and thymine base pairs, some of them in alternating order (1). It is of particular interest that AT-rich regions separate functional domains in eukaryotic DNA (3). For example, in the yeast genome coding sequences tend to be clustered, while long AT-rich sequences are found between them. They are also frequent in transposable elements (4).

A very suggestive example is the TATA-box bound to the TATA-binding protein (1, 2, 5, 6) where a very highly distorted B conformation with Watson–Crick base pairing has been found. Analysis of the structure adopted by the TATA-box revealed a form of double helix named TA-DNA (7). Other possible DNA conformations have been proposed for alternating AT polynucleotides (8). At low temperatures (0–25°C), it appears that AT-rich oligonucleotides may have several conformational forms (9–11). In the case of poly[d(A-T)], it has been suggested that the C form of DNA is stabilized at low temperature (12). The polymorphism of AT regions suggested by all these studies prompted us to determine the structure of an oligonucleotide with 100% A·T base pairs. Although in the last 20 years a considerable amount of work on oligodeoxynucleotide crystals either alone or in complexes with proteins and drugs has been carried out, no structural information is available on long sequences entirely composed of A·T base pairs. In all previous studies, the presence of CG flanking bases may influence the conformation of the AT regions. Thus, we decided to determine the structure of the deoxynucleotides d(ApTpApTpApT) and d(ApTpAp^{Br}UpApT). Surprisingly, we discovered an antiparallel double helix fully stabilized by Hoogsteen base pairs.

Hoogsteen base pairs have been known for more than 40 years (13). Soon after the model of DNA was proposed (14) several attempts were made to demonstrate that Watson–Crick pairing was favored by isolated bases. However, a different scheme of hydrogen bonds between adenine and thymine was found, first described by Hoogsteen (13) and later observed in other related structures, as reviewed by Voet and Rich (15). In Hoogsteen base pairs the N7 face of adenine is hydrogen bonded to thymine. Such interactions were postulated in U(A·U) triple helices (16). Hoogsteen base pairs have been also found in chemically modified nucleic acids (17, 18). Isolated Hoogsteen base pairs have been reported in some protein/DNA complexes (1) and occasionally in RNA (19). Our finding demonstrates an alternative conformation for duplex DNA and opens the question of the possible biological implication of Hoogsteen DNA in molecular processes. A complete duplex with Hoogsteen base pairs has been crystallized.

Methods

Synthesis, Crystallization, and Data Processing. The self-complementary deoxyhexanucleotides d(ApTpApTpApT) and d(ApTpAp^{Br}UpApT) were synthesized on an automatic synthesizer by the phosphoramidite method and purified by gel filtration and reverse-phase HPLC. The ammonium salt of the hexamers was prepared by ion exchange chromatography. Crystallization attempts were first carried out with the unmodified sequence d(ApTpApTpApT). Crystals were obtained under the same conditions as described below for the brominated derivative, but diffracted only to a 2.8-Å resolution. Attempts to solve the structure by molecular replacement were not successful, so we decided to obtain crystals from the brominated derivative to solve the structure by multiwavelength anomalous dispersion. The thin, platelike crystals of d(ApTpAp^{Br}UpApT) were grown at 13°C by the hanging-drop method. The crystallization solution contained 0.7 mM duplex, 3 mM spermine, 9 mM KCl, 25 mM sodium cacodylate at pH 6, and 37% (vol/vol) 2-methyl-2,4-pentanediol (MPD). The drop was equilibrated against a reservoir solution at 38% (vol/vol) MPD. No divalent ion has been used. Crystals appeared after ≈3 weeks. Diffraction data for both crystals (unmodified and brominated) were measured with cryo-cooling at 110 K at the European Synchrotron Radiation Facility at the BM14 (United Kingdom/Spanish Collaborating Research Group beamline), processed and scaled by using HKL2000 (20). Both crystals belong to space group $P2_1$ ($Z = 2$) and show practically identical unit cell dimensions. Data were collected at four wavelengths around the Br absorption edge (Table 1). But because of fine structure around the edge, two different "point of inflection" data sets were collected, along with one corresponding to the F″ peak and a short wavelength "remote" data set. The data were scaled together by using SCALEIT (21), and there was no noticeable radiation decay of the crystal between the first and fourth data sets.

Phasing and Structure Refinement. The four Br sites were readily identifiable from the anomalous and dispersive Patterson maps, and verified by anomalous difference Fourier. Heavy atom refinement and phasing was carried out with MLPHARE (21). The data collected on the second inflection point ($\lambda = 0.9189$ Å) were taken as reference during phasing. Solvent flattening and

Data deposition: The atomic coordinates have been deposited in the Protein Data Bank, http://ebi.ac.uk (PDB ID code: 1gqu).

†Present address: Division of Structural Biology, Wellcome Trust Centre for Human Genetics, University of Oxford, Oxford OX3 7BN, United Kingdom.

¶To whom reprint requests should be addressed. E-mail: subirana@eq.upc.es.

The publication costs of this article were defrayed in part by page charge payment. This article must therefore be hereby marked "*advertisement*" in accordance with 18 U.S.C. §1734 solely to indicate this fact.

Table 1. Data collection and refinement statistics

	d(ApTpApTpApT)	d(ApTpAp^{Br}UpApT)			
Data collection					
λ, Å	0.91850	0.919	0.919352	0.9189	0.8550
Cell parameters, Å	$a = 23.66$, $b = 48.37$, $c = 32.23$, $\beta = 92.82°$		$a = 23.96$, $b = 48.95$, $c = 32.24$, $\beta = 93.27°$		
Space group	$P2_1$		$P2_1$		
Resolution range, Å	30.0–2.82		30.0–2.50		
Unique reflections	1,763	2,591	2,594	2,587	2,599
Completeness (%) $I/\sigma \geq 2$	78.6 (48.4)*	90.3 (68.6)	87.5 (65.2)	87.9 (66.9)	83.9 (60.0)
Overall redundancy†	4.9	10.4	5.3	5.2	5.6
R_{merge}‡ (%)	0.083 (0.299)	0.060 (0.175)	0.053 (0.128)	0.058 (0.133)	0.074 (0.268)
R_{merge} anom§ (%)		0.059 (0.126)	0.035 (0.132)	0.047 (0.140)	0.056 (0.169)
Completeness anom¶, %		89.2	87.7	87.9	84.0
R_{Cullis}‖ (centric/anom.)		0.66/0.49	0.70/0.88	—	0.44/0.73
Phasing power** (acentric/centric)		1.68/1.08	1.75/1.08	—	2.87/2.18

d(ApTpAp^{Br}UpApT) refinement statistics ($\lambda = 0.9190$ Å, 15–2.5 Å)	
No. DNA atoms	480
No. water molecules	48
R_{work}††, %	22.0
No. reflections work set ($F > 0$)	2,307
R_{free},‡‡ %	23.4
No. reflections free set ($F > 0$)	240
rmsd bond lengths, Å	0.0089
rmsd bond angles, °	1.17

*Hereafter values in parentheses correspond to the outermost resolution shell.
†Total reflections registered divided by the unique ones.
‡$R_{merge} = \Sigma_{hkl}\Sigma_i|I_i(hkl) - \langle I(hkl)\rangle|/\Sigma_{hkl}\Sigma_i I_i(hkl)$, calculated for the whole data set.
§R_{merge} anomalous $= \Sigma_{hkl}\Sigma_i|I_i(hkl\pm) - \langle I(hkl)\rangle|/\Sigma_{hkl}\Sigma_i I_i(hkl\pm)$.
¶Percentage of reflections with a Bijvoet pair.
‖R_{Cullis} is the mean residual lack of closure error divided by the dispersive difference.
**Phasing power = rms ($|F_H|/E$), where F_H is the heavy atom amplitude and E is the residual lack of closure error.
††R factor $= \Sigma_{hkl}||F_o(hkl)| - k|F_c(hkl)||/\Sigma_{hkl}|F_o(hkl)|$.
‡‡R factor of reflections used for crossvalidation in the refinement.

density modification lead to an electron density map at 2.5 Å, with a combined figure of merit (MLPHARE) of 0.87. A preliminary Watson–Crick double helix was traced with the O program (22) using the bromine sites as fingerprints for the palindromic sequence. Because of the higher resolution of the derivative crystal (Table 1), the built model was refined against the peak anomalous data rescaled as native. Refinement with the CNS (23) package followed standard protocols. The maximum likelihood function was used as target function and the refinement was monitored with a random free data set for crossvalidation. We first conservatively tried to interpret the experimental multiwavelength anomalous dispersion electron density map by using standard Watson–Crick pairing, but the fit to the electron density was poor and refinement did not converge. The poor convergence of the refinement and the disruption of the N6···O4 hydrogen bond of all adenine·thymine Watson–Crick pairs (either restrained or not) suggested the alternative Hoogsteen pairing scheme. The new model was refined successfully (Fig. 1*A*). A preliminary rigid body refinement followed by torsion-angle molecular dynamics, group *B*-factor refinement, conjugate gradient minimization, and manual rebuilding in O with σ_A-weighted difference Fourier maps was carried out until all of the extrahelical bases were located unambiguously. No restraint was applied to hydrogen bonding. The model, once completed (Fig. 1*B*), showed an internal pseudo-twofold axis perpendicular to the helix axis, announced also by the self-rotation calculation. However, the NCS operator was not taken into account during the refinement steps.

Results

Description of the Crystal Structure. The crystal structure is shown in Fig. 1*B*. This structure is, to our knowledge, the longest sequence with only AT bases that has ever been studied by single-crystal x-ray crystallography. The asymmetric unit consists of two hexamer duplexes, which are stacked one on top of another, forming a pseudocontinuous double helix. One hexamer pair is fully Hoogsteen double helical (blue in the figure), but the other hexamer pair (red and green in Fig. 1*B*) has four base pairs in a Hoogsteen double helical configuration, whereas the two terminal AT nucleotides are nonhelical. These nucleotides are positioned in the grooves of either the same or neighbor duplexes.

The crystal is formed by parallel columns of stacked duplexes. The nonhelical bases form bridges between such columns, which stabilizes the crystal lattice. On the other hand, there are large solvent channels that run along the x direction of the crystal.

Structural Features of Hoogsteen DNA. Some of the conformational parameters of the duplex structure are given in Table 2. A comparison between Hoogsteen DNA and an ideal B form DNA with the same sequence is presented in Fig. 2. The overall features of the double helix are strikingly similar in both cases: both are antiparallel. The twist values given in Table 2 show that, in Hoogsteen DNA, there is an average of 10.6 base pairs per turn, as in B DNA. The sugar pucker (as measured by the δ angle, also given in Table 2) lies in the C2′-*endo* region typical of B-DNA, with the exception of the terminal thymine 12, which is C3′-*endo*. On projection, the base pairs are moved away from the helical axis, as is apparent from Fig. 2. As a result, because the C1′–C1′ distance is shorter, the double helical phosphodiester backbone has similar dimensions as the B form of DNA; the phosphate–phosphate distances across the minor groove are in

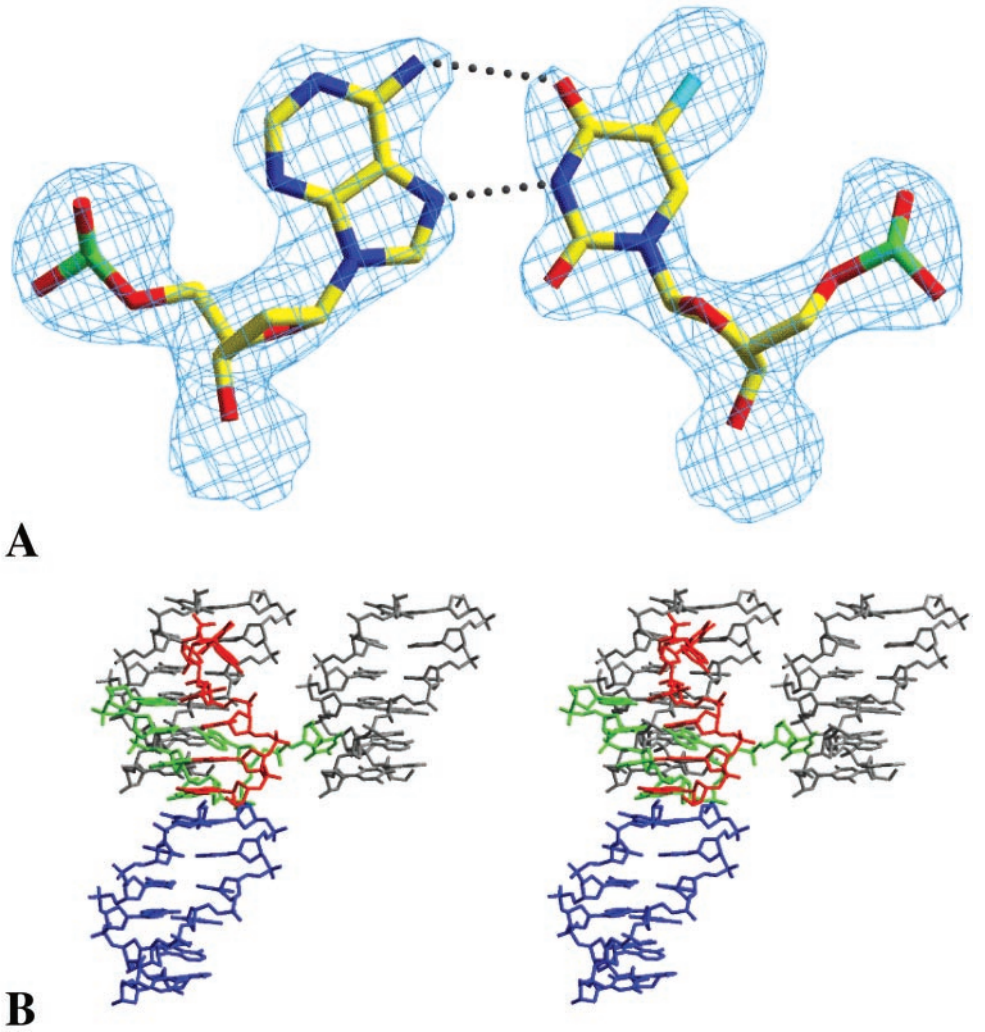

Fig. 1. Views of Hoogsteen DNA. (*A*) ($2F_o - F_c$) electron density map (base pair A3·^{Br}U10) of the refined structure (1.1 σ). The Hoogsteen base pairs fit the electron density map throughout the structure. Note that the adenine base has now two hydrogen-bond acceptor atoms (N1 and N3) in the major groove side and none in the minor groove, whereas in the B form there is one in each groove (N7 and N3 respectively). (*B*) Stereo pair of the crystal structure of d(ApTpAp^{Br}UpApT). The asymmetric unit consists of a fully helical hexamer duplex (in blue) plus another hexamer duplex (red and green) with four base pairs in a duplex configuration, whereas the two terminal bases of each strand are extrahelical. The terminal thymines are located in the minor grooves of neighbor duplexes (in gray), whereas one terminal adenine (green) fits into the minor groove of the tetramer duplex. The two duplexes are stabilized by Hoogsteen base pairs, as shown in *A*. All figures have been prepared with SETOR (24).

the range 9.3–11.1 Å, similar to those frequently found in narrow minor groove tracks of B form DNA. In fact, the shorter C1′–C1′ distance across a base pair, in the range 7.9–8.4 Å (Table 2), is a further proof of the presence of Hoogsteen base pairs in our structure. This value corresponds to the values found in isolated Hoogsteen base pairs (13, 15, 17, 18), whereas the distance is 10.85 Å in standard Watson–Crick base pairs.

A characteristic feature of Hoogsteen DNA is the *syn* conformation of the purine base A; all its glycosidic angles χ (Table 2) lie in the *gauche*$^+$ region. This feature is also found for the purine base G in Z-DNA (25). The pattern of hydrogen bonding sites is also unique, because Hoogsteen DNA has two adenine hydrogen bond acceptor sites (N1 and N3) in the major groove, whereas in B form DNA there is a single hydrogen bond acceptor (N7). The interactions with ions, solvent, and proteins should therefore be quite different in either case. In the minor groove side, the difference in hydrogen bonding potential is very apparent in Fig. 3*A*, where the Hoogsteen DNA hexamer is compared with the central sequence of d(CGTATATACG) (26). Both have a deep and narrow minor groove, but in the B-DNA structure, the electronegative N3 atom of adenine (in blue) is clearly apparent, whereas no nitrogen is present in the minor groove of Hoogsteen DNA.

An additional difference with B form DNA lies in the fact that there is no alternation in twist values (Table 2), which is obvious (26, 27) in alternating AT sequences of B form DNA. Base-pair stacking is also different: in B form DNA, there is a good overlap of the bases in the AT step and little overlap in the TA step, whereas the opposite is found in Hoogsteen DNA.

Hoogsteen DNA Hydration. A number of well-defined water molecules have been found along the phosphate backbone and on the major groove of the double helix, in particular close to the N3 atom of adenines. Some of these molecules are involved in a bridge between the latter atom and a phosphate group, as shown in Fig. 3*B*. The latter interaction contributes to the stability of Hoogsteen base pairs. It should be noted that the minor groove, partially occupied by three extrahelical bases, has very little room left to build a spine of hydration; a single water molecule is found between the nonhelical thymines that occupy

Table 2. Conformational parameters of Hoogsteen DNA

Atom	Angle, degrees							Twist	C1′–C1′, Å
	α	β	γ	δ	ε	ζ	χ		
A1	—	—	48	144	−177	−90	61	34.0	8.1
T2	−59	−177	42	128	−169	−118	−113	36.5	7.9
A3	37	−174	−63	152	167	−90	83	35.5	7.9
^{Br}U4	−52	−173	43	137	−165	−104	−106	37.4	8.4
A5	−55	169	36	128	−173	−114	91	32.7	8.2
T6	−56	169	51	135	—	—	−92		8.2
A7	—	—	52	146	−176	−83	54		
T8	−66	−178	41	128	−166	−121	−109		
A9	−45	159	45	129	168	−95	73		
^{Br}U10	−53	−165	43	136	−159	−110	−105		
A11	28	−158	−74	148	−169	−93	80		
T12	−77	165	56	83	—	—	−125		

Only values for the hexamer duplex are given. The tetramer has similar values. α–χ are the standard conformational angles of the DNA backbone. The other parameters have been calculated with the FREEHELIX program found in the Nucleic Acid Database (http://ndbserver.rutgers.edu/).

the minor groove. In fact, the Hoogsteen pairing mode, which flips over the adenine base around the glycosidic bond, confers to the minor groove a less electronegative environment, which should favor the interaction with hydrophobic groups. Such interaction is evident from the insertion of nonhelical thymines and adenines found in the crystal structure, as shown in detail in Fig. 4. Hydrophobic amino acid side chains in proteins might interact in a similar way with Hoogsteen DNA.

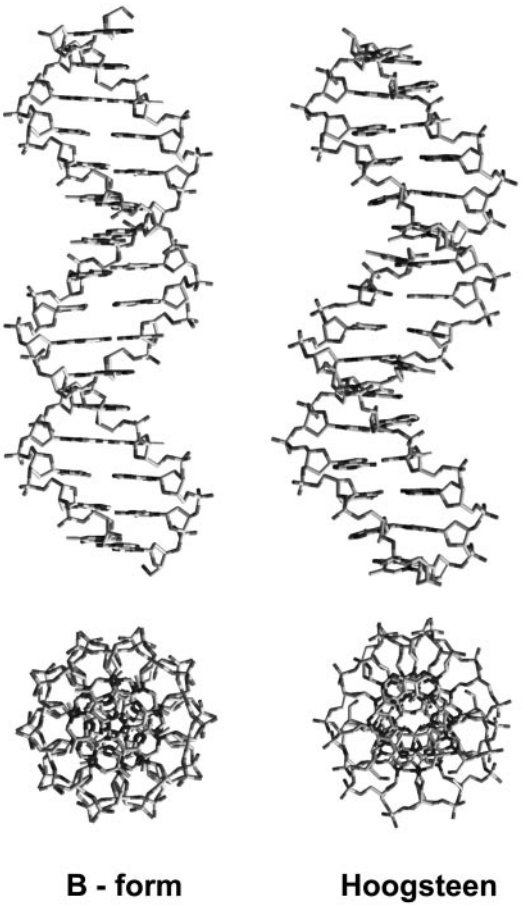

Fig. 2. Comparison of ideal B form (*Left*) with Hoogsteen DNA (*Right*). Hoogsteen DNA has been obtained from a hexamer/tetramer/hexamer stack as found in the crystal structure.

Comparison with Parallel DNA and Triple-Helical Structures. The Hoogsteen duplex shows adenines in *syn* conformation and thymines in the normal *anti* conformation (Fig. 1*A*). Reverse Hoogsteen pairing is not possible, because this would place the phosphodiester chains in a different relative position, not compatible with the x-ray data. The duplex is clearly antiparallel, as is apparent from the electron density distribution along the phosphodiester polymer chains; thus, it is not related to parallel DNA, which differs in the relative orientation of the phosphodiester chains. Parallel DNA may show different hydrogen bonding schemes, either reverse Watson–Crick (28) or Hoogsteen (29), as found in our structure. However, parallel DNA appears to be only marginally stable and rearranges easily into conventional structures (30).

Hoogsteen DNA is also clearly different with respect to triple-helical structures (31). In the T(A·T) case (32), the adenine is always in the normal *anti* conformation; T and A form the Hoogsteen pair in the parallel orientation and the reverse Hoogsteen pair in the antiparallel orientation. In the A(A·T) case, hydrogen bonding of adenine in the third strand is always with adenine of the Watson–Crick base pair. Thus the Hoogsteen DNA structure described in the present paper is not a component of the triple-stranded helical structures described thus far, which are always based on the addition of a third strand on to a standard antiparallel Watson–Crick double helix.

Discussion

After describing the main features of this double helical form of DNA, we may ask why we have detected it in this particular case. The conditions used for crystallization do not play any apparent role to help the formation of Hoogsteen base pairs; they are similar to those used in many oligonucleotide crystals. The only variants were a low temperature (13°C) and no divalent cations present. It is precisely under the latter conditions that a conformational variability of A·T base pairs has been described (9–12). Unfortunately, NMR experiments (9–11) were carried out with sequences that also contain C·G base pairs; no NMR data are available on oligonucleotides that contain only A·T base pairs. Although Watson–Crick base pairing is always preserved, the NMR data (9–11) cannot exclude the presence of a minor Hoogsteen component. In the case of poly[d(A-T)] (12), it has been suggested that C form DNA is formed at premelting temperatures, but from the evidence presented it cannot be excluded that Hoogsteen DNA might be responsible for the changes in circular dichroism observed. It is interesting to note that in the latter case the low-temperature form was also favored

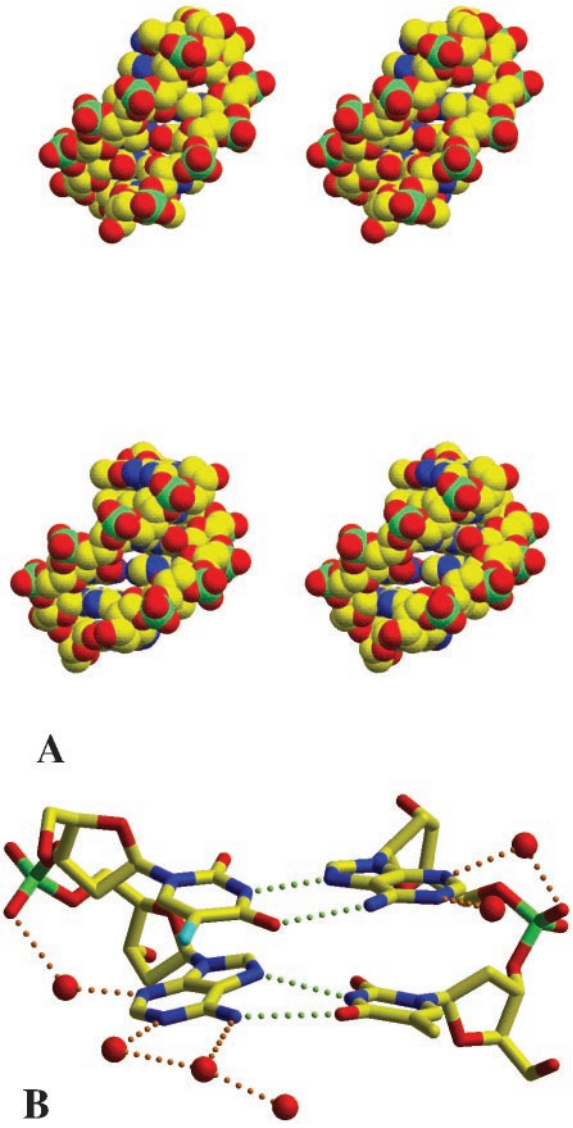

Fig. 3. Groove structure of Hoogsteen DNA. (*A*) Comparison of minor groove structure (stereo pairs). The central AT-rich region of d(CGTATATACG) (26) in the B form (*Lower*) is compared with the Hoogsteen hexamer (*Upper*). Both have a narrow minor groove. The presence of the N3 hydrogen bond acceptor group of adenine (blue) is clearly apparent in B-form DNA. (*B*) A detail of major groove hydration. Some water molecules (red spheres) are hydrogen bonded both to the N3 atom of adenine and to a phosphate oxygen.

by the absence of divalent cations, which were also absent in our crystallization conditions.

The formation of A·T Hoogsteen base pairs in our crystal structure appears to be cooperative, because such base pairing has never been detected in mixed sequence oligonucleotide crystals. Thus, longer $(AT)_n$ sequences might also show Hoogsteen base pairs, even within intact genomes. The striking similarity of Hoogsteen DNA with standard B form DNA (Fig. 2) will not allow detection of the formation of Hoogsteen form of DNA by the standard methods used in DNA analysis, such as electrophoresis.

It is worth comparing the structure of $d(ApT)_3$ reported here with that of Z-DNA (25), which is also found in an alternating sequence, $d(CpG)_n$. In fact, there are reports (33) that suggest that $d(ApT)_n$ could also adopt the Z form. An important difference is that Z-DNA requires a change in the sense of the

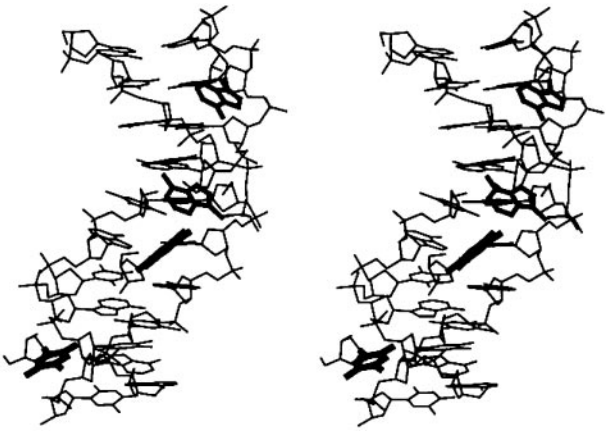

Fig. 4. Stereo pair of Hoogsteen DNA as found in the crystal. Two thymines from neighbor molecules enter the minor groove of the hexamer duplex (lower part). An adenine is found in the minor groove of the tetramer duplex (upper part), whereas the other extra helical adenine lies on the major groove of the hexamer. The three bases in the minor groove form tight van der Waals contacts plus a single hydrogen bond with a base in the groove.

helix. Hoogsteen DNA might be an intermediate in an eventual B-to-Z transition, because the adenine bases are already flipped over as in Z-DNA.

We should also note that the structures of some shorter AT sequences have been reported, but the results obtained are different from those presented here. For example, the structure of d(ApTpApT) was determined several years ago (34, 35) and showed Watson–Crick base pairs in a nonstandard conformation. Hoogsteen base pairs were suggested (36) to interpret the fiber diffraction pattern of d(TpA), but the helical model that was suggested was left handed. Fibers of poly[d(AT)] have also been studied. They show on dehydration a different form of DNA known as D form (8), with eight base pairs per turn. This form is certainly not what we have found. It remains an open question whether the D form will also turn out to use the Hoogsteen base pairing scheme.

An important question is whether Hoogsteen DNA has sequence specificity. In principle, C·G base pairs can also acquire the Hoogsteen conformation, but it is considered to be less stable. In that case, only two hydrogen bonds between the bases are used and cytosine needs to be protonated. However, the results of Patikoglou *et al.* (1) show that occasional C·G Hoogsteen base pairs may be found in protein/DNA complexes. In the latter, case the N2 amino group of guanine was hydrogen bonded to a phosphate group, so that guanine maintains its three hydrogen bonds. Thus, it cannot be excluded that general sequence DNA fragments might show the Hoogsteen conformation in special cases.

Although Hoogsteen geometry has been found occasionally (1, 19), we may finally ask whether Hoogsteen DNA will be found in biological systems. Some proteins might specifically interact with Hoogsteen pairs, because the pattern of hydrogen-bond acceptors and overall geometry are changed when compared with B-form DNA. In TATA-box/protein complexes some CG residues show Hoogsteen base pairs (1). Interestingly in that case, hydrophobic phenylalanine residues are found in the minor groove. A unique feature of our crystal structure is the presence of extrahelical adenines and thymines in the minor groove (Fig. 4), which may favor a more hydrophobic environment and thus stabilize Hoogsteen base pairs. We can expect that AT-rich sequences in the presence of minor groove hydrophobic binding substances (such as appropriate amino acid side chains) might show the Hoogsteen conformation, although at this point it is not

clear if this is a necessary requirement for Hoogsteen DNA to be formed.

We thank G. Minasov for preliminary crystallization experiments and I. Fita for superb advice throughout this work. We also thank J. Bordas and staff BM14 at the European Synchrotron Radiation Facility: J. Juanhuix, D. Beltran, and A. Labrador. The advice of M. Frank-Kamenetskii was most helpful for the analysis of our results and their presentation. This work has been supported by grants from the Generalitat de Catalunya, the Ministerio de Educación y Ciencia, and the European Commission (Marie Curie Fellowship to N.G.A.A. and access to the Grenoble Synchrotron).

1. Patikoglou, G. A., Kim, J. L., Sun, L., Yang, S.-H., Kodadek, T. & Burley, S. K. (1999) *Genes Dev.* **13,** 3217–3230.
2. Juo, Z. S., Chiu, T. K., Leiberman, P. M., Baikalov, I., Berk, A. J. & Dickerson, R. E. (1996) *J. Mol. Biol.* **261,** 239–254.
3. Moreau, J., Maschat, M. F., Kejzlarova-Lepesant, J., Lepesant, J.-A. & Scherrer, K. (1982) *Nature (London)* **295,** 260–262.
4. Oosumi, T., Garlick, B. & Belknap, W. R. (1995) *Proc. Natl. Acad. Sci. USA* **92,** 8886–8890.
5. Kim, J. L., Nikolov, D. B. & Burley, S. K. (1993) *Nature (London)* **365,** 520–527.
6. Kim, Y., Geiger, J. H., Hanh, S. & Sigler, P. B. (1993) *Nature (London)* **365,** 512–520.
7. Guzikevich-Guerstein, G. & Shakked, Z. (1996) *Nat. Struct. Biol.* **3,** 32–37.
8. Davies, D. R. & Baldwin, R. L. (1963) *J. Mol. Biol.* **6,** 251–255.
9. Lefèvre, J.-F., Lane, A. N. & Jardetzky, O. (1988) *Biochemistry* **27,** 1086–1094.
10. Schmitz, U., Sethson, I., Egan, W. M. & James, T. L. (1992) *J. Mol. Biol.* **227,** 510–531.
11. McAteer, K., Ellis, P. D. & Kennedy, M. A. (1995) *Nucleic Acids Res.* **23,** 3962–3966.
12. Brahms, S., Brahms, J. & Van Holde, K. E. (1976) *Proc. Natl. Acad. Sci. USA* **73,** 3453–3457.
13. Hoogsteen, K. (1959) *Acta Crystallogr.* **12,** 822–823.
14. Watson, J. D. & Crick, F. H. (1953) *Nature (London)* **171,** 737–738.
15. Voet, D. & Rich, A. (1970) *Prog. Nucl. Acid Res. Mol. Biol.* **10,** 183–265.
16. Felsenfeld, G., Davies, D. R. & Rich, A. (1957) *J. Am. Chem. Soc.* **79,** 2023–2024.
17. Hakoshima, T., Fukui, T., Ikehara, M. & Tomita, K.-I. (1981) *Proc. Natl. Acad. Sci. USA* **78,** 7309–7313.
18. Isaksson, J., Zamaratski, E., Maltseva, T. V., Agback, P., Kumar, A. & Chattopadhyaya, J. (2001) *J. Biomol. Struct. Dyn.* **18,** 783–806.
19. Leontis, N. B. & Westhof, E. (1998) *Quart. Rev. Biophys.* **31,** 399–455.
20. Otwinoski, Z. & Minor, W. (1997) *Methods Enzymol.* **276,** 307–326.
21. Collaborative Computational Project No. 4 (1994) *Acta Crystallogr. D* **50,** 760–763.
22. Jones, T. A., Zou, J. Y., Cowan, S. W. & Kjeldgaard, M. (1991) *Acta Crystallogr. A* **47,** 110–119.
23. Brünger, A. T., Adams, P. D., Clore, G. M., DeLano, W. L., Gros, P., Grosse-Kunstleve, R. W., Jiang, J. S., Kuszewski, J., Nilges, M., Pannu, N. S., *et al.* (1998) *Acta Crystallogr. D* **54,** 905–921.
24. Evans, S. V. (1993) *J. Mol. Graph.* **11,** 134–138.
25. Wang, A. H.-J., Quigley, G. J., Kolpak, F. J., Crawford, J. L., van Boom, J. H., van der Marel, G. & Rich, A. (1979) *Nature (London)* **282,** 680–686.
26. Abrescia, N. G. A., Malinina, L., Fernández, L. G., Huynh-Dinh, T., Neidle, S. & Subirana, J. A. (1999) *Nucleic Acids Res.* **27,** 1593–1599.
27. Yuan, H., Quintana, J. & Dickerson, R. E. (1992) *Biochemistry* **31,** 8009–8021.
28. Van de Sande, J. H., Ramsing, N. B., Germann, M. W., Elhorst, W., Kalisch, B. W., von Kitzing E., Pon, R. T., Clegg, R. C. & Jovin, T. M. (1988) *Science* **241,** 551–557.
29. Liu, K., Miles, H. T., Frazier, J. & Sasisekharan, V. (1993) *Biochemistry* **44,** 11802–11809.
30. Bhaumik, S. R., Chary, K. V. R., Govil, G., Liu, K. & Miles, H. T. (1997) *Biopolymers* **41,** 773–784.
31. Frank-Kamenetskii, M. D. & Mirkin, S. M. (1995) *Annu. Rev. Biochem.* **64,** 65–95.
32. Cheng, Y.-K. & Pettitt, B. M. (1992) *J. Am. Chem. Soc.* **114,** 4465–4474.
33. Bourtayre, P., Liquier, J., Pizzorni, L. & Taillandier, E. (1987) *J. Biomol. Struct. Dyn.* **5,** 97–104.
34. Viswamitra, M. A., Kennard, O., Jones, P. G., Sheldrick, G. M., Salisbury, S., Falvello, L. & Shakked, Z. (1978) *Nature (London)* **273,** 687–688.
35. Viswamitra, M. A., Shakked, Z., Sheldrick, J. G. M., Salisbury, S. A. & Kennard, O. (1982) *Biopolymers* **21,** 513–533.
36. Radwan, M. M. & Wilson, H. R. (1982) *Int. J. Biol. Macromol.* **4,** 145–149.